

Surface confined quantum well state in MoS₂(0001) thin film

Jia-Tao Sun (孙家涛),^{1,a)} S. R. Song,¹ S. Meng,¹ S. X. Du,¹ F. Liu,² and H. J. Gao¹

¹Institute of Physics, Chinese Academy of Sciences, Beijing 100190, China

²Department of Materials Science and Engineering, University of Utah, Salt Lake City, Utah 84112, USA

(Received 13 July 2015; accepted 11 October 2015; published online 22 October 2015)

Surface confined quantum well state (scQWS) is a QWS confined around the surface of a thin film whose electronic energy is smaller than the work function of the film. The scQWS is rather rare in most thin films. Here, we show the existence of scQWS in thin films of transition metal dichalcogenides, MoS₂. Signatures of scQWS are identified as the overall downward band dispersion in the bulk gap of 2H-MoS₂ thin film at larger binding energy range. These scQWSs are also characterized with a Shockley-type surface state having an inverse parabolic decay into the film and a symmetric (asymmetric) distribution of projected charge density at the two surfaces of odd-layer (even-layer) films. Our findings of scQWS in MoS₂ shed some light on understanding the electronic properties of 2D materials with implications in future 2D electronic devices. © 2015 AIP Publishing LLC. [<http://dx.doi.org/10.1063/1.4934610>]

Research on graphene and other two-dimensional (2D) atomic crystals,^{1,2} such as transition metal dichalcogenides and boron nitride, is rising to be one of the leading topics in condensed matter physics because of a variety of unusual properties originating from the quantum confinement in comparison with their three-dimensional matrix. When the isolated atomic planes are stacking in a way of layer by layer into van der Waals (referred to be vdw hereafter) structures, they can reveal unusual properties and phenomena unexplored before. Many fundamental physics not present in individual 2D crystal is widely expected to emerge in vdw structures with atomically thin barriers and quantum wells (QWs).^{3,4}

The remarkable effect is that the electrons confined in thin films lead to QW state (QWS).^{5,6} The electrons confined by the finite barrier involve multiple reflections between two film boundaries. When the thickness of potential barrier is comparable with the de Broglie wavelength of the electrons, it leads to quantized energy level and the standing wave of electronic states takes place. Due to the presence of boundary between crystal surface and vacuum, the finite barrier for QWSs leads to the following Bohr-Sommerfeld quantization rule (also known as phase accumulation rule)⁷

$$2\kappa(E)d + \phi(E) = 2n\pi, \quad (1)$$

where ϕ is the binding energy and E is the dependent phase shift at the boundary. Here, the momentum κ is the binding energy dependent as well. n is the principal quantum number of a quantum well state with film thickness of d . For free electron gas confined in one-dimensional box, the quantized energy levels follow $E = \hbar^2\kappa^2/2m^*$, where m^* is the effective mass for a free electron. The allowed wave vector k for quantum well states is given by $\kappa = n\pi/L$. Thus, we have the power-law scaling $E \propto 1/m^*L^2$. This is a special form of Bohr-Sommerfeld rule.⁷ If the electronic energy is roughly in the bulk gap, the electron cannot propagate inside the bulk crystal and will be reflected backward forming quantum well resonance (QWr).⁸ If the energy of an electron is smaller

than the work function, the electron is therefore confined by the crystal surface potential. Therefore, the confined electronic states around the film surface will decay in a parabolic scaling like QWS. This leads to surface confined QWS (scQWS), which has characteristics of both quantum well state⁹ and crystal Shockley-type surface state (SSS).¹⁰

The SSS is ubiquitous in 2D confined geometry of materials, which include closely packed surfaces of noble metals such as Au(111),¹⁰ Ag(111),^{11,12} Cu(111),¹³ and Pt(111).¹⁴ The wave function of a solid takes the form of $\psi_0 = u(r)e^{ik_x x + ik_y y + ik_z z}$, where $u(r)$ is the periodic part of the Bloch wave function. In the metal thin films, the periodicity of a crystal solid is broken by the presence of surface. Then, k_z in the general Bloch wave function is replaced by a complex number λ . The SSS is non-degenerate due to the coupling of opposite surfaces for smaller film thickness. The energy separation between the non-degenerate electronic band follows $E \propto e^{-Re(\lambda)L}$,¹⁵ which indicates that the reciprocal interaction between opposite surfaces will decay exponentially. With the increasing film thickness, the SSS electronic states become degenerate and are characterized by the parabolic band dispersion with positive effective mass in the gaps of the projected bulk states. Moreover, the projected charge density for these SSS accumulates around the film surface, and decay exponentially into the thin films, which is strikingly different from the *parabolic decay* in scQWS. Moreover, the binding energy and wave function of the SSS are independent of the film thickness. Similarly, these properties of the scQWS are independent of the film thickness as well.

Normally, the scQWS is rare in thin films of conventional noble metals due to the delocalized electron gas. Here, we show the existence of crystal surface confined QWS in thin films of molybdenum dichalcogenides by performing density functional theory (DFT) calculations. The planar averaged charge density for scQWS is localized around the surface, just like the SSS. Different from the exponential decay of the SSS in 2DEG system, however, an inverse power-law scaling is found in much thicker MoS₂ films, signifying the origin of QWS. Furthermore, the projected

^{a)}jtsun@iphy.ac.cn

charge density shows a symmetric (asymmetric) distribution at the two surfaces of odd-layer (even-layer) films.

The electronic ground-state calculations have been carried out within density functional theory formalism as implemented in the VASP code.¹⁶ The interaction between valence electrons and ion cores is described by projector augmented wave (PAW) method.¹⁷ The exchange-correlation functional is described by local density approximation (LDA).^{18,19} The plane-wave kinetic energy cutoff of 400 eV has been employed for the expansion of wave function. We used slab models to represent the crystal surfaces in DFT calculations. Each slab has vacuum of thickness of 20 Å to prevent spurious interaction between them due to the periodic boundary condition. Structural optimizations for all the studied MoS₂ slabs were performed by fixing the in-plane lattice constant to that of experimental bulk MoS₂ ($a_0 = 3.166$ Å).²⁰ All ions in the studied MoS₂ slabs were then relaxed until the Hellmann-Feynman forces were less than 10 meV/Å.

Figures 1(a) and 1(b) show the atomic structures of two-layer MoS₂ thin films as indicated by shallow orange areas. Each MoS₂ monolayer consists of one layer of Mo atoms (blue) sandwiched by two layers of S atoms (green) in such a way that each Mo atom is coordinated by six S atoms in a trigonal prismatic geometry and each S atom is coordinated by three Mo atoms. The symmetry group of monolayer MoS₂ is D_{3h} , which contains the discrete symmetries C_3 (trigonal rotation), σ_v (reflection by the yz plane), σ_h (reflection by the xy plane), and any of their products.

It is well established that the electronic structures of MoS₂ thin films (Fig. 1(d)) evolve from direct semiconductor in monolayer limit to indirect semiconductor in the multilayer case. The detailed evolution of the band gap of the MoS₂ films with the inverse of film thickness is shown in Fig. 2(a). The black (red) dotted line is the evolution of direct (indirect) band gap of the MoS₂ film at K point (from Γ point to Q valley). Both lines (black and red lines) show similar trend of the band gap evolution for the MoS₂ films. The calculated direct band gap for monolayer MoS₂ is 1.9 eV, which is smaller than that by including the quasiparticle correction.²⁰ This is due to the well-known problem of local density approximation in DFT framework, which usually underestimates the band gap of solid materials,¹⁹ but will not affect our analysis here. Eight-layer MoS₂ film is a semiconductor

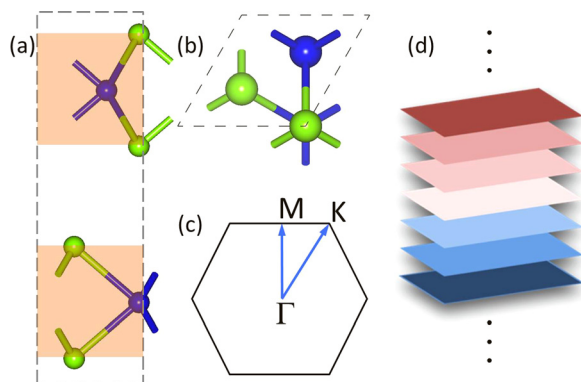


FIG. 1. Atomic structures and Brillouin zone of molybdenum disulfide. (a) Side view and (b) top view of two-layer MoS₂. (c) The two dimensional Brillouin zone with high symmetry points. (d) The schematics of multilayer MoS₂.

with an indirect band gap of about 0.69 eV because of the indirect electronic hopping from Γ point and the so-called Q valley between Γ point and K point (Fig. 2(b)) as shown in the first Brillouin zone (Fig. 1(c)).

To investigate the quantum well state of MoS₂ thin films, the band structures of the eight-layer MoS₂ film are superposed on the projected band structures of bulk MoS₂, as shown by the gray background. Closer inspection of the band structures of the eight-layer MoS₂ film (Fig. 2(b)) shows that the two energy bands with energy separation Δ_E from the reciprocal surface interaction appear in the gap of the projected bulk states roughly located at the -1.45 eV below the valence band maximum. A magnified view of both energy bands is shown in Fig. 2(c). It is found that both bands show a valley-like dispersion with a small scale of the Brillouin zone. More interestingly, the valley-like band dispersion will become flatter, and a protrusion-like band dispersion will appear eventually in this small region with the increasing film thickness. Beyond the valley region, both bands originate from the QWS of the eight-layer MoS₂ slab, when the momentum of the scQWS states is far away from the Γ point. With the increasing thickness of the MoS₂ films, the separation Δ_E (black dots in Fig. 2(d)) between two electronic states at the Γ point decreases and degenerates eventually. This is expectedly due to the vanishing interaction of both the surfaces, which indicates that both the bands have similar properties of the Shockley-type SS.

As mentioned above, the SSS exhibits an exponential scaling as a function of the film thickness, namely, the energy separation Δ_E decays exponentially as characterized by the real part of λ . So, the calculated energy splitting Δ_E is first fit by an exponential curve. Surprisingly, the calculated data Δ_E cannot be fit well with an exponential curve. Instead, the calculated data can be nicely fit by a second-order power-law scaling function, as shown in Fig. 2(d) (blue line). This indicates that the energy separation Δ_E does not decay with film thickness steeply in an exponential fashion as expected for the SSS, but decay slower in an inverse parabolic scaling, characteristic of quantum well state. This leads us to believe that the band dispersion projected in the bulk gap of the MoS₂ thin film have the electronic origin from the QWS rather than the SSS. Since these states with the inverse parabolic decay are localized at the surface, we further characterize them as surface confined QWS. The calculated effective mass in the valley in the vicinity of the Γ point is 2.8 in unit of free electron mass m_0 , which is also confirmed with hybrid functional calculations.²¹ Obviously, the calculated effective mass deviates significantly from that of free electron mass. We have projected the orbital contributed density of state to both the bands, as shown in Fig. 2(c). It is found that both the bands are mainly contributed by d_{z^2} -orbital of molybdenum. The “heavy” effective mass of both bands could be most probably the reason for their special properties.

As mentioned above, the surface confined quantum well states as found in MoS₂ slabs are located deep in energy at about 1.4 eV below the valence band maximum. This means that an electron in occupied states has to overcome 1.4 eV plus the ionic potential to reach the Fermi level. It has been reported that work function of thick MoS₂ films (more than 3 layers) is 4.59 eV (Ref. 22), indicating that it is hard for an

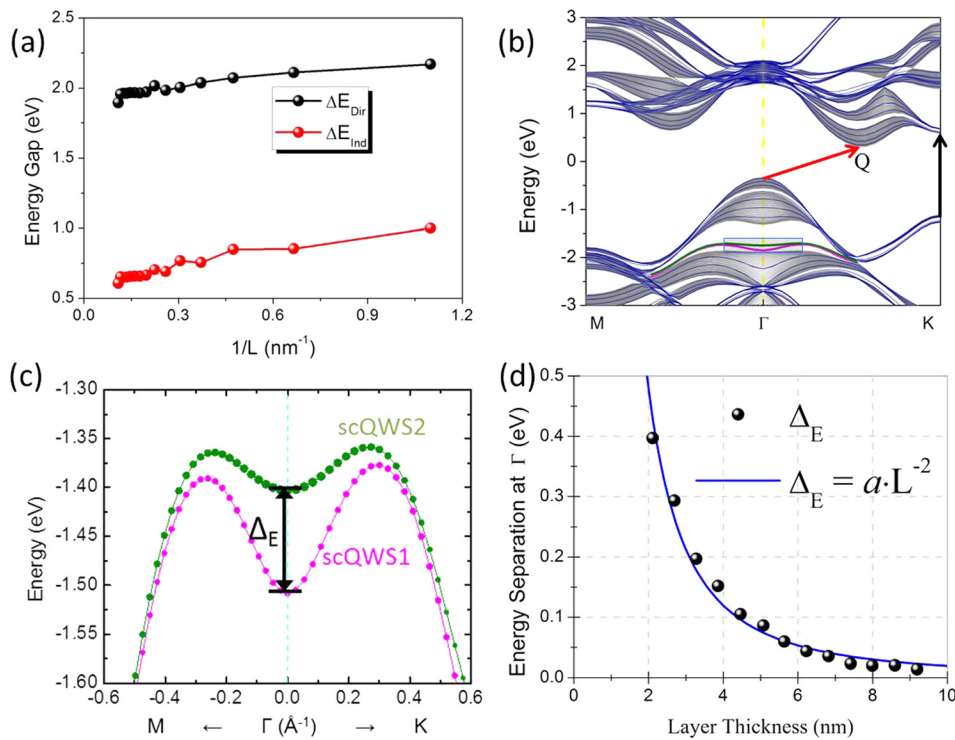


FIG. 2. (a) Inverse layer thickness ($1/L$) dependence of direct (black dots) and indirect (red dots) band gap. (b) The band structure (blue line) of eight-layer MoS₂ plus the projected bulk band (gray shaded background). The Fermi level is moved to the top of valence band. The surface confined quantum well states (scQWSs) are shown as green and pink lines for opposite surfaces. (c) The magnified view of an eight-layer MoS₂ film extracted from the small squared region of panel (b). The circle size indicates the contribution of the projected Mo d_{z^2} orbitals. The color lines indicate opposite surface planes. (d) The thickness dependence of energy separation Δ (black dots) is fitted by a power law curve (blue line) using least-square algorithm.

electron to escape to the vacuum. Consequently, the electrons inside the MoS₂ thin films experience a very strong surface confinement potential leading to the formation of scQWS.

The term scQWS means that although these states originate from the bulk QWSs, their charge distribution is confined around the crystal surfaces. It is interesting to find out how the scQWSs evolve from the bulk QWSs to become the surface confined ones. To answer this question, we have calculated the planar averaged charge density of the two scQWS and two QWS in the vicinity of the Γ point for the even (fourteen-) and odd (fifty-) layer MoS₂ slabs as examples. As shown in Figs. 3(a) and 4(a), the bulk QWS1 and QWS2 have tiny beating patterns contributing to a slowly varying envelope function, which is characterized by a longer wave-length comparable with the thickness of MoS₂ thin film. This is the $n=1$ order of QWS according to the Bohr-Sommerfeld rule (Eq. (1)). The different beating patterns between QWS1 and QWS2 are due to the various contributions among the plane wave components. For scQWSs, the envelope function does not show such tiny beating patterns (green and pink lines in Figs. 3(a) and 4(a)). The projected charge density of plane-wave eigenfunctions is localized to the surface, which seems to be similar with the SSS. However, a closer inspection of the projected charge density around the crystal surface of the MoS₂ thin film reveals a slow decay with a penetration depth of about 4 or 5 layers, which is significantly different from the steep exponential decay usually seen in noble metal surfaces. Therefore, the projected charge density provides again direct evidence that what we obtained are indeed QWSs originating from the surface confinement.

The envelope function for the normal QWSs and the charge density accumulation around the crystal surface for the scQWSs are also clearly visible in a fifteen-layer MoS₂ film. Particularly, the accumulated charge density of the scQWS shows symmetric patterns, which are in direct contrast with

the asymmetric patterns seen in a fourteen-layer MoS₂ film. The distinction of the charge density pattern, so called odd-even oscillation, is obviously due to the phase shift (Eq. (1)) in the geometric structures of the MoS₂ film. The momentum dependence of planar averaged charge density for the normal QWS and the scQWS provides an opportunity to study the evolution of the surface confined QWSs in the MoS₂ slabs (Figs. 3(b) and 4(b)). The scQWS in even-layer (odd-layer) showing an asymmetric (symmetric) momentum dependence of the projected charge density indicates isotropic band dispersion around the center of Brillouin zone.

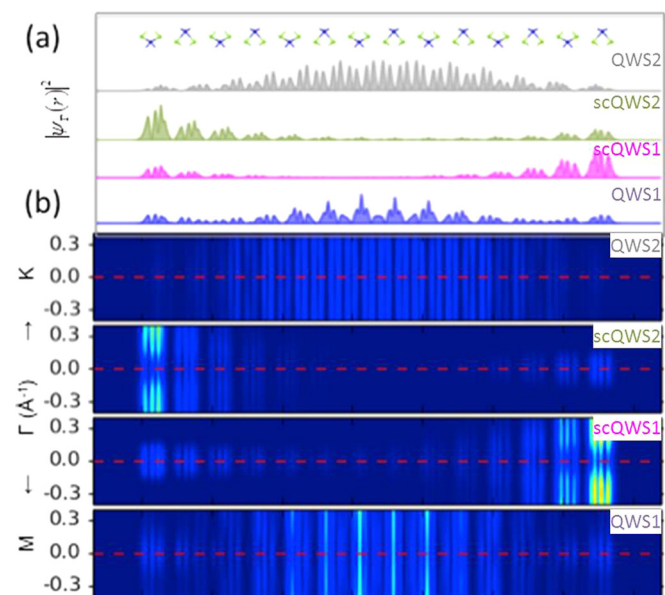


FIG. 3. (a) Γ point and (b) momentum dependence of planar averaged charge density of a fourteen-layer MoS₂ slab in the Brillouin zone for two bulk QWSs and two scQWSs. The atomic structures of a fourteen-layer MoS₂ slab are superimposed, where blue and green dots symbolize the Mo atoms and S atoms, respectively.

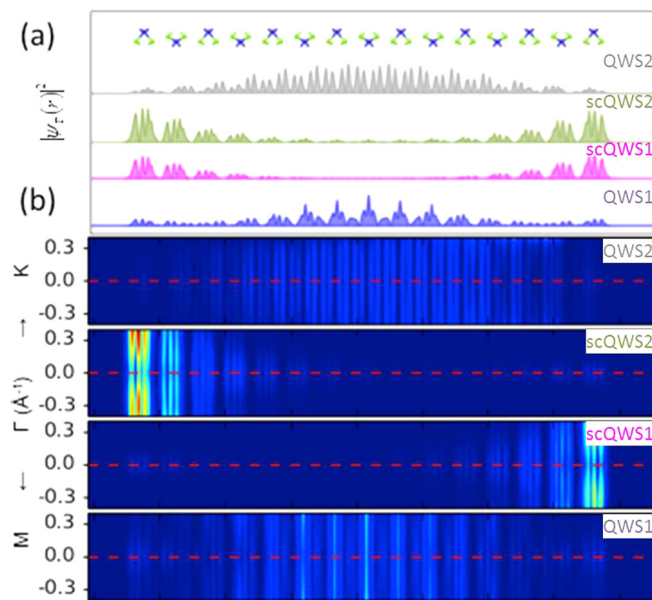


FIG. 4. (a) Γ point and (b) momentum dependence of planar averaged charge density of a fifteen-layer MoS_2 slab in the Brillouin zone for two bulk QWSs and two scQWSs. The atomic structures of a fifteen-layer MoS_2 slab are superimposed, where blue and green dots symbolize the Mo atoms and S atoms, respectively.

In conclusion, a rare scQWS has been found in the MoS_2 thin films. Different from the SSS with delocalized electron in conventional transition metals, the scQWSs in the MoS_2 film show a larger effective mass of $2.8m_0$. Our work may shed some light on understanding some puzzling and inconclusive experimental observations in the MoS_2 films, such as exciton with high binding energy,^{23,24} transport of intercalated lithium atoms,^{25,26} *p*-type metal contacts with MoS_2 (Refs. 27–30), etc.

This work was supported by the National Basic Research Program of China (Grant No. 2013CBA01600), the National Natural Science Foundation of China (Grant No. 61306114), and “Strategic Priority Research Program (B)” of the Chinese Academy of Sciences (Grant No. XDB07030100), and the startup funding from the Institute of Physics, Chinese Academy of Sciences.

¹A. K. Geim and K. S. Novoselov, *Nat. Mater.* **6**, 183 (2007).

²Q. H. Wang, K. Kalantar-Zadeh, A. Kis, J. N. Coleman, and M. S. Strano, *Nat. Nanotechnol.* **7**, 699 (2012).

- ³H. Min, R. Bistritzer, J. J. Su, and A. H. MacDonald, *Phys. Rev. B* **78**, 121401 (2008).
- ⁴L. A. Ponomarenko, A. K. Geim, A. A. Zhukov, R. Jalil, S. V. Morozov, K. S. Novoselov, I. V. Grigorieva, E. H. Hill, V. V. Cheianov, V. I. Fal’ko, K. Watanabe, T. Taniguchi, and R. V. Gorbachev, *Nat. Phys.* **7**, 958 (2011).
- ⁵R. Shankar, *Principles of Quantum Mechanics* 2nd ed. (Plenum Press, New York, 2011).
- ⁶M. I. Elinson, V. A. Volkov, V. N. Lutskij, and T. N. Pinsker, *Thin Solid Films* **12**, 383 (1972).
- ⁷T. C. Chiang, *Surf. Sci. Rep.* **39**, 181 (2000).
- ⁸E. Ogando, N. Zabala, E. V. Chulkov, and M. J. Puska, *J. Phys.: Condens. Matter* **20**, 315002 (2008).
- ⁹F. K. Schulte, *Surf. Sci.* **55**, 427 (1976).
- ¹⁰S. LaShell, B. A. McDougall, and E. Jensen, *Phys. Rev. Lett.* **77**, 3419 (1996).
- ¹¹D. Popović, F. Reinert, S. Hüfner, V. G. Grigoryan, M. Springborg, H. Cercellier, Y. Fagot-Revurat, B. Kierren, and D. Malterre, *Phys. Rev. B* **72**, 045419 (2005).
- ¹²H. Cercellier, C. Didiot, Y. Fagot-Revurat, B. Kierren, L. Moreau, D. Malterre, and F. Reinert, *Phys. Rev. B* **73**, 195413 (2006).
- ¹³A. Tamai, W. Meevasana, P. D. C. King, C. W. Nicholson, A. de la Torre, E. Rozbicki, and F. Baumberger, *Phys. Rev. B* **87**, 075113 (2013).
- ¹⁴N. Levy, S. A. Burke, K. L. Meaker, M. Panlasigui, A. Zettl, F. Guinea, A. H. Castro Neto, and M. F. Crommie, *Science* **329**, 544 (2010).
- ¹⁵P. F. Zhang, Z. Liu, W. Duan, F. Liu, and J. Wu, *Phys. Rev. B* **85**, 201410 (R) (2012).
- ¹⁶G. Kresse and J. Hafner, *Phys. Rev. B* **47**, 558 (1993); **49**, 14251 (1994); G. Kresse and J. Furthmüller, *Comput. Mater. Sci.* **6**, 15 (1996); *Phys. Rev. B* **54**, 11169 (1996).
- ¹⁷P. E. Blöchl, *Phys. Rev. B* **50**, 17953 (1994); G. Kresse and D. Joubert, *ibid.* **59**, 1758 (1999).
- ¹⁸J. P. Perdew and A. Zunger, *Phys. Rev. B* **23**, 5048 (1981).
- ¹⁹It is known that local density approximation notably overestimates the binding and underestimates the energy gap or energy splitting in Van der Waals (vdW) stacked nanostructures. Nevertheless, the fundamental physics of surface confined quantum well state in MoS_2 slabs discussed in this work is solid.
- ²⁰A. Ramasubramaniam, *Phys. Rev. B* **86**, 115409 (2012).
- ²¹H. Peelaers and C. G. Van de Walle, *Phys. Rev. B* **86**, 241401 (2012).
- ²²O. Ochedowski, K. Marinov, N. Scheuschner, A. Poloczek, B. K. Bussmann, J. Maultzsch, and M. Schleberger, *Beilstein J. Nanotechnol.* **5**, 291 (2014).
- ²³Z. Ye, T. Cao, K. O’Brien, H. Zhu, X. Yin, Y. Wang, S. G. Louie, and X. Zhang, *Nature* **513**, 214 (2014).
- ²⁴A. R. Klots, A. K. M. Newaz, B. Wang, D. Prasai, H. Krzyzanowska, J. Lin, D. Caudel, N. J. Ghimire, J. Yan, B. L. Ivanov, K. A. Velizhanin, A. Burger, D. G. Mandrus, N. H. Tolc, S. T. Pantelides, and K. I. Bolotin, *Sci. Rep.* **4**, 6608 (2014).
- ²⁵N. Imanishi, M. Toyoda, Y. Takeda, and O. Yamamoto, *Solid State Ionics* **58**, 333 (1992).
- ²⁶A. Ambrosi, Z. Sofer, and M. Pumera, *Small* **11**, 605 (2015).
- ²⁷N. Kaushik, A. Nipane, F. Basheer, S. Dubey, S. Grover, M. M. Deshmukh, and S. Lodha, *Appl. Phys. Lett.* **105**, 113505 (2014).
- ²⁸N. R. Pradhan, D. Rhodes, Q. Zhang, S. Talapatra, M. Terrones, and P. M. Ajayan, *Appl. Phys. Lett.* **102**, 123105 (2013).
- ²⁹J. Kang, W. Liu, and K. Banerjee, *Appl. Phys. Lett.* **104**, 093106 (2014).
- ³⁰S. Walia, S. Balendhran, Y. Wang, R. A. Kadir, A. S. Zoofakar, P. Atkin, J. Z. Ou, S. Sriram, K. Kalantar-zadeh, and M. Bhaskaran, *Appl. Phys. Lett.* **103**, 232105 (2013).